



# Optimization of T-cell Receptor–Modified T Cells for Cancer Therapy

Dylan J. Drakes<sup>1</sup>, Sarwish Rafiq<sup>2</sup>, Terence J. Purdon<sup>3</sup>, Andrea V. Lopez<sup>3</sup>, Smita S. Chandran<sup>3,4,5</sup>, Christopher A. Klebanoff<sup>3,4,5,6</sup>, and Renier J. Brentjens<sup>1,3,4,7</sup>

## ABSTRACT

T-cell receptor (TCR)–modified T-cell gene therapy can target a variety of extracellular and intracellular tumor-associated antigens, yet has had little clinical success. A potential explanation for limited antitumor efficacy is a lack of T-cell activation *in vivo*. We postulated that expression of proinflammatory cytokines in TCR-modified T cells would activate T cells and enhance antitumor efficacy. We demonstrate that expression of interleukin 18 (IL18) in tumor-directed TCR-modified T cells provides a superior proinflammatory signal than expression of interleukin 12 (IL12). Tumor-targeted T cells secreting IL18 promote persistent and functional effector T cells and a proin-

flammatory tumor microenvironment. Together, these effects augmented overall survival of mice in the pmel-1 syngeneic tumor model. When combined with sublethal irradiation, IL18-secreting pmel-1 T cells were able to eradicate tumors, whereas IL12-secreting pmel-1 T cells caused toxicity in mice through excessive cytokine secretion. In another xenograft tumor model, IL18 secretion enhanced the persistence and antitumor efficacy of NY-ESO-1–reactive TCR-modified human T cells as well as overall survival of tumor-bearing mice. These results demonstrate a rationale for optimizing the efficacy of TCR-modified T-cell cancer therapy through expression of IL18.

## Introduction

T-cell activation is dependent upon T-cell receptor (TCR) engagement with peptides processed and presented in the context of a MHC (signal 1) and costimulation (signal 2; refs. 1, 2). Signal 2 is derived from CD28, 4-1BB, or OX-40 molecules (1, 2). T cells receiving both signals develop effector function and secrete proinflammatory cytokines. Without signal 2, T cells become anergic (3–5). Proinflammatory cytokines interleukin-12 (IL12) or type I interferon can act as signal 3 to heighten the effector function of T cells (6–10). Optimizing T-cell stimulation through this proinflammatory pathway may augment antitumor efficacy of tumor-targeted T cells.

Several clinical trials have tested autologous isolated tumor-infiltrating lymphocytes (TIL) or TCR-modified T cells for cancer therapy (11). Although these approaches can target extracellular and intracellular tumor-associated antigens, trial results have been modest (12–18). Strategies to enhance the potency of these TCR T cells include increasing the affinity of the TCR to tumor-associated antigens, although this sometimes has adverse effects (12, 19, 20). One promising method to enhance the efficacy of tumor-directed T

cells is providing a stimulatory signal to TIL or TCR-modified T cells. Lack of T-cell activation may contribute to failure of T-cell therapies if tumor cells downregulate costimulatory molecule expression (21, 22).

Chimeric antigen receptor (CAR) T cells carry an antigen-recognition domain fused to a costimulatory and CD3 $\zeta$  domain, through which the cell receives both signals 1 and 2. This configuration eliminates the need for additional stimulation provided by antigen-presenting cells (APC) or tumor cells (23, 24). With CAR T-cell therapy, the single-chain variable fragment (scFv) in the CAR is directed toward extracellular antigens and not intracellular antigens that might be presented extracellularly within the context of an MHC. For certain tumor types, especially solid tumors, there are few extracellular antigens that can be distinguished from those of healthy tissues and specifically targeted by CARs, limiting potential targets. TCR-modified T cells, however, can be redirected to tumor-specific targets, including intracellular antigens, but are limited overall by a lack of T-cell activation (11, 21, 22). We hypothesized that proinflammatory cytokine modifications could activate T cells and enhance the efficacy of tumor-directed TCR-modified T cells. Here we explore approaches to enhance TCR-modified T cells through genetic engineering with proinflammatory IL12 or IL18 cytokines.

Clinical trials of patients treated with systemic recombinant IL12 have shown modest efficacy, although results have been limited by toxicities (25). Treatment with recombinant IL18 did not cause toxicities but showed limited clinical responses (26). Directing cytokines to the tumor site may alleviate toxicity and enhance antitumor responses. IL18-dependent signaling occurs through a heterodimeric receptor (IL18R $\alpha$  and IL18R $\beta$ ). Most immune cell types express IL18R $\alpha$ . IL18R $\beta$  is commonly expressed on T cells, dendritic cells, macrophages, and other myeloid cells (27, 28). Thus, adoptive transfer of IL18-secreting T cells could enhance the activity of T cells while modulating the tumor microenvironment.

CAR T-cell function has been augmented by IL12 and IL18 cytokine secretion, with IL12 under the control of an internal ribosome entry site (IRES) element to limit toxicities (29–31). The pmel-1 TCR transgenic murine melanoma model has been used to show that IL12

<sup>1</sup>Department of Pharmacology, Weill Cornell Graduate School of Medical Sciences, New York, New York. <sup>2</sup>Department of Hematology and Medical Oncology, Winship Cancer Institute of Emory University School of Medicine, Atlanta, Georgia. <sup>3</sup>Department of Medicine, Memorial Sloan Kettering Cancer Center, New York, New York. <sup>4</sup>Center for Cell Engineering, Memorial Sloan Kettering Cancer Center, New York, New York. <sup>5</sup>Parker Institute for Cancer Immunotherapy, New York, New York. <sup>6</sup>Weill Cornell Medical College, New York, New York. <sup>7</sup>Cellular Therapeutics Center, Memorial Sloan Kettering Cancer Center, New York, New York.

**Note:** Supplementary data for this article are available at Cancer Immunology Research Online (<http://cancerimmunolres.aacrjournals.org/>).

**Corresponding Author:** Renier J. Brentjens, Memorial Sloan Kettering Cancer Center, Box #242, 1275 York Avenue, New York, NY 10065. Phone: 212-639-7053; Fax: 212-772-8441; E-mail: [brentjer@mskcc.org](mailto:brentjer@mskcc.org)

Cancer Immunol Res 2020;XX:XX–XX

doi: 10.1158/2326-6066.CIR-19-0910

©2020 American Association for Cancer Research.

enhances T-cell function when combined with a lymphodepleting preconditioning regimen (32–34). Using a syngeneic and xenograft melanoma model, we show that expression of IL18 in TCR-modified T cells provides a potent and durable proinflammatory signal to activate T cells and enhance T-cell persistence and antitumor efficacy demonstrating that antitumor efficacy of TCR-modified T cells is optimized through engineering with IL18.

## Materials and Methods

### Contact for reagent and resource sharing

Further information and requests for resources and reagents should be directed to and will be fulfilled by the lead contact, R. J. Brentjens.

### Experimental model and subject details

#### Animal models

Mice were bred and housed under specific pathogen-free conditions in the animal facility of Memorial Sloan Kettering Cancer Center (MSKCC; New York, NY). Wild-type C57BL/6, pmel-1[B6.Cg-Thy1<sup>a</sup>/CyTg(TcraTcrb)8Rest/J], CD80/86<sup>-/-</sup> (B6.129S4-CD80<sup>tm1Shr</sup>Cd86<sup>tm2Shr</sup>/J), IL18R<sup>-/-</sup> (B6.129P2-Il18r1<sup>tm1Aki</sup>/J), and NSG (NOD.Cg-Prkdc<sup>scid</sup>IL2rg<sup>tm1Wjl</sup>/SzJ) mice were purchased from Jackson laboratories. Six- to 8-week-old gender-matched mice challenged with tumor were measured with calipers to confirm equal tumor load and randomized to different treatment groups one day before treatment. Mice were euthanized when tumor growth led to a volume greater than 1,000mm<sup>3</sup> by  $V = \frac{\pi}{6}(ab^2)$  where  $a$  is the longest length and  $b$  is the shortest length. The investigator was blinded when assessing the outcome.

#### Cell lines

Phoenix-ECO packaging cells (catalog no. CRL-3214) purchased from ATCC and 293 galv9 packaging cells (courtesy of the Sadelain lab, MSKCC, New York, NY) were maintained in DMEM supplemented with 10% heat-inactivated FBS nonessential amino acids, 2 mmol/L L-glutamine, 1% penicillin/streptomycin. The B16F10 cell line, a kind gift from Dr. Jedd Wolchok (MSKCC, New York, NY) in 2016, and A375 and SK-Mel5 human melanoma lines, a kind gift from Dr. David Scheinberg (MSKCC, New York, NY) in 2018, were modified to express GFP-firefly luciferase for killing assays. Cell lines were kept in culture for up to 2 months. All tumor cell lines were maintained in RPMI1640 supplemented with 10% heat-inactivated FBS, nonessential amino acids, 1 mmol/L sodium pyruvate, 10 mmol/L HEPES, 2 mmol/L L-glutamine, 1% penicillin/streptomycin, 11 mmol/L glucose, and 2 μmol/L 2-mercaptoethanol. Cell lines were not reauthenticated in the past year but were routinely tested for potential *Mycoplasma* contamination with Lonza MycoAlert Detection Kit (LT07-318).

#### Generation of retroviral constructs

Plasmids encoding the mCD19t construct in the SFG γ-retroviral vector (35) were used to transfect gpg29 fibroblasts (H29) with the ProFection Mammalian Transfection System (Promega) according to the manufacturer's instructions to generate vesicular stomatitis virus G-glycoprotein–pseudotyped retroviral supernatants. These retroviral supernatants were used to construct stable Moloney murine leukemia virus–pseudotyped retroviral particle-producing Phoenix-ECO cell lines or 293 galv9 cell lines. The SFG-mCD19t, SFG-mCD19tmIL12, and SFG-mCD19tmIL18 vector were constructed by restriction enzyme digest using the cDNA of mCD19 protein truncated to exclude

the intracellular domain alone or with either the fusion gene encoding murine IL12 (mIL12; refs. 29, 30, 36; provided by Dr. Alan Houghton and Dr. Jedd Wolchok, MSKCC, New York, NY) or the mature form of murine IL18 (mIL18). mIL12 was preceded by an IRES element and mIL18 was preceded by a picornavirus 2a element (P2A) self-cleaving peptide. For xenograft experiments, an optimized NY-ESO-1-directed TCR, 1G4, α- and β-chain sequence was provided by the Klebanoff Lab (37–39) and cloned into the SFG γ-retroviral vector alone or in combination with an equine 2A element followed by a signal peptide and the mature, processed form of human IL18 (hIL18). Nucleotide sequences are provided in Supplementary Fig. S1.

### T-cell isolation and retroviral transduction

Mice were euthanized and their spleens were harvested. Following tissue dissociation and red blood cell lysis, T cells were activated with CD3/CD28 Dynabeads at a bead:cell ratio of 1:2 (Invitrogen). Cells were expanded *in vitro* by culturing in RPMI1640 supplemented with 10% heat-inactivated FBS, nonessential amino acids, 1 mmol/L sodium pyruvate, 10 mmol/L HEPES, 2 mmol/L L-glutamine, 1% penicillin/streptomycin, 11 mmol/L glucose, 2 μmol/L 2-mercaptoethanol, and 100 IU/mL of recombinant human IL2 (Prometheus Therapeutics & Diagnostics). 24 and 48 hours after initial expansion, T cells were spinoculated with viral supernatant collected from Phoenix-ECO cells as described previously (40). Human T cells were activated and transduced as described previously (41). Peripheral blood mononuclear cells were isolated from leukopacks (New York Blood Center, New York, NY), activated with 2 μg/mL phytohemagglutinin and 100 IU/mL of IL2, and cultured in RPMI1640 supplemented with 10% heat-inactivated FBS, 2 mmol/L L-glutamine, and 1% penicillin/streptomycin for 2 days prior to transduction. 48 and 72 hours after initial expansion, murine and human T cells were transduced by centrifugation on RetroNectin (Takara Clontech) plates with retroviral supernatant from viral packaging cells.

### Cytotoxicity assays

**24-hour quantitative cytotoxicity assay:** Cytolytic capacity of murine and human T cells was assessed through luciferase killing assay (42).  $5 \times 10^4$  target tumor cells expressing firefly luciferase were cocultured with adoptively transferred T cells at various effector-to-target ratios in triplicates in black-walled 96-well plates (Thermo Fisher Scientific) in a total volume of 200 μL of cell media. Target cells alone were plated at the same cell density to determine the maximal luciferase expression as a reference (max signal). 24 hours later, 75 ng of D-Luciferin (Gold Biotechnology) dissolved in 5 μL of PBS was added to each well. Emitted luminescence of each sample (sample signal) was detected in a Spark plate reader (Tecan) and quantified using the SparkControl software (Tecan). Percent lysis was determined as  $[1 - (\text{sample signal}/\text{max signal})] \times 100$ .

**Ex vivo cytotoxicity assay:**  $5 \times 10^4$  B16F10 GFP/ffLuc were cocultured at a 1:1 ratio with  $5 \times 10^4$  Thy1.1<sup>+</sup> T cells excised from tumors on day 6 and day 13 post T-cell infusion and sorting via FACS, in a total volume of 200 μL of cell media. Target cells alone were plated at the same cell density to determine the maximal luciferase expression as a reference (max signal). 24 hours later, 75 ng of D-Luciferin (Gold Biotechnology) dissolved in 50 μL of PBS was added to each well. Emitted luminescence of each sample (sample signal) was detected in a Spark plate reader (Tecan) and quantified using the SparkControl software (Tecan). Percent lysis was determined as  $[1 - (\text{sample signal}/\text{max signal})] \times 100$ .

### Adoptive transfer of TCR-modified T cells

For syngeneic tumor studies, C57BL/6 mice were inoculated subcutaneously with  $5 \times 10^5$  B16F10 melanoma tumor cells on day 10. On day 1, tumors were measured with calipers and mice with equal tumor burden were selected for treatment. Mice were then randomized into different treatment cohorts and on days 0, 7, and 14, mice were treated with  $5 \times 10^6$  T cells intravenously. For irradiation studies, the above protocol was followed in addition to sublethally irradiating the tumor-bearing mice with 5 Gy total body irradiation on day 1. For xenograft tumor studies,  $5 \times 10^6$  A375 (NY-ESO-1<sup>+</sup>) tumor cells were injected subcutaneously into NSG mice on day 10 and then treated with  $2.5 \times 10^6$  adoptively transferred human T cells intravenously on day 0.

### Cell isolation for *ex vivo* analyses

$5 \times 10^6$  armored or control modified pmel-1 T cells were infused and either 6 or 13 days after T-cell infusion, tumor samples were excised on days 6 and 13 post T-cell infusion and mechanically dissociated using a 150  $\mu$ mol/L metal mesh and glass pestle in 2.5% FBS/PBS and passed through a 100  $\mu$ mol/L cell strainer. The homogenate was spun down at 1,500 RPM for 5 minutes at 4°C to pellet the cells. Cells were counted and an aliquot was stained for flow cytometry analysis. For the remaining sample, red blood cell lysis was achieved with an ACK (Ammonium-Chloride-Potassium) Lysing Buffer (Lonza). The cells were washed with PBS, FACS sorted, and used for subsequent analyses.

### *In vitro* and *ex vivo* cytokine secretion analysis

To analyze *in vitro* and *ex vivo* T-cell cytokine production, T cells and antigen-positive tumor cells were cocultured in a 1:1 ratio for 24 hours in a 96-well round-bottom plate in 200  $\mu$ L of media. The supernatant was collected and analyzed for cytokines on a Luminex IS100 instrument. Luminex FlexMap3D system and Luminex Xponent 4.2 (Millipore Corporation) were used to detect cytokines.

### Serum T-cell and cytokine analysis

Whole blood was collected from mice and serum was prepared by allowing the blood to clot during centrifugation at 14,000 RPM for 30 minutes at 4°C. Red blood cell lysis was achieved with an ACK (Ammonium-Chloride-Potassium) Lysing Buffer (Lonza). T cells were washed with PBS and used for subsequent flow cytometry analysis. Serum was analyzed for cytokines with Luminex.

### *In vitro* tumor cell analysis

To assess CD80 and CD86 surface expression on tumor cells, the cells were collected, surface stained, and analyzed by flow cytometry.

### Flow cytometry and FACS sorting

Flow cytometric analyses were performed using 10-color Gallios B43618 (Beckman Coulter) and 14-color Attune NxT (Thermo Fisher Scientific) instruments to acquire data. Data were analyzed using FlowJo (Tree Star). DAPI (0.5 mg/mL, Sigma-Aldrich) or a LIVE/DEAD fixable yellow fluorescent dye (Thermo Fisher Scientific) were used to exclude dead cells in all experiments. Flow cytometry gating strategies are provided in Supplementary Fig. S2. Antibodies to the following mouse proteins were used for flow cytometry: CD3e (eBioscience, clone 145-2C11), CD3 (BioLegend, 17A2), CD4 (eBioscience, GK1.5), CD4 (eBioscience, RM4-5), CD8 $\alpha$  (eBioscience, 53-6.7), CD11b (eBioscience, M1/70), CD11c (eBioscience, N418), CD19 (eBioscience, eBio1D3), CD25 (eBioscience, PC61.5), CD44

(eBioscience, IM7), CD45 (BioLegend, 30-F11), CD62L (Invitrogen, MEL-14), CD80 (eBioscience, 16-10A1), CD86 (eBioscience, GL1), CD90.1 (Thy-1.1; Invitrogen, HIS51), CD206 (Invitrogen, MR5D3), CD218a (IL18R; eBioscience, P3TUNYA), CD223 (Lag-3; eBioscience, C9B7W), CD279 (PD-1; Invitrogen, J43), CD366 (TIM3; Invitrogen, 8B.2C12), F4/80 (eBioscience, BM8), FoxP3 (eBioscience, FJK-16s), Ly-6C (eBioscience, HK1.4), Ly-6G/Ly-6C (Gr-1; eBioscience, RB6-8C5), MHC Class II I-Ab (Invitrogen, AF6-120.1), and NK1.1 (eBioscience, PK136). Antibodies to the following human proteins were used for flow cytometry: CD3 [Invitrogen, clone S4.1 (7D6)], CD4 (eBioscience, OKT4), CD8 (BioLegend, SK1), CD80 (Invitrogen, MEM-233), CD86 (Invitrogen, BU63), HLA-A2 (Invitrogen, BB7.2), and HLA-A\*02:01 NY-ESO-1 (SLLMWITQC) iTag Tetramer (MBL). Quantification of total cell numbers by flow cytometry was done using 123count eBeads Counting Beads (Thermo Fisher Scientific). Staining of Foxp3 was done using the Foxp3/Transcription factor staining buffer set from eBioscience. All antibodies were purchased from BioLegend, BD Biosciences, eBioscience, Invitrogen, or MBL. Sorting of splenocytes after tissue processing was done using a BD FACSAria under sterile conditions.

### Statistical analysis

All statistical analyses were performed using GraphPad Prism software (GraphPad). Data points represent biological replicates and are shown as the mean  $\pm$  SEM or mean  $\pm$  SD as indicated in the figure legends. Statistical significance was determined using an unpaired two-tailed Student *t* test, one-way ANOVA, or two-way ANOVA as indicated in the figure legends. Mann-Whitney test was used to determine statistical significance for tumor volume growth curves. The log-rank (Mantel-Cox) test was used to determine statistical significance for overall survival in mouse survival experiments. Significance was assumed with \*,  $P < 0.05$ ; \*\*,  $P < 0.01$ ; \*\*\*,  $P < 0.001$ ; and \*\*\*\*,  $P < 0.0001$ .

### Study approval

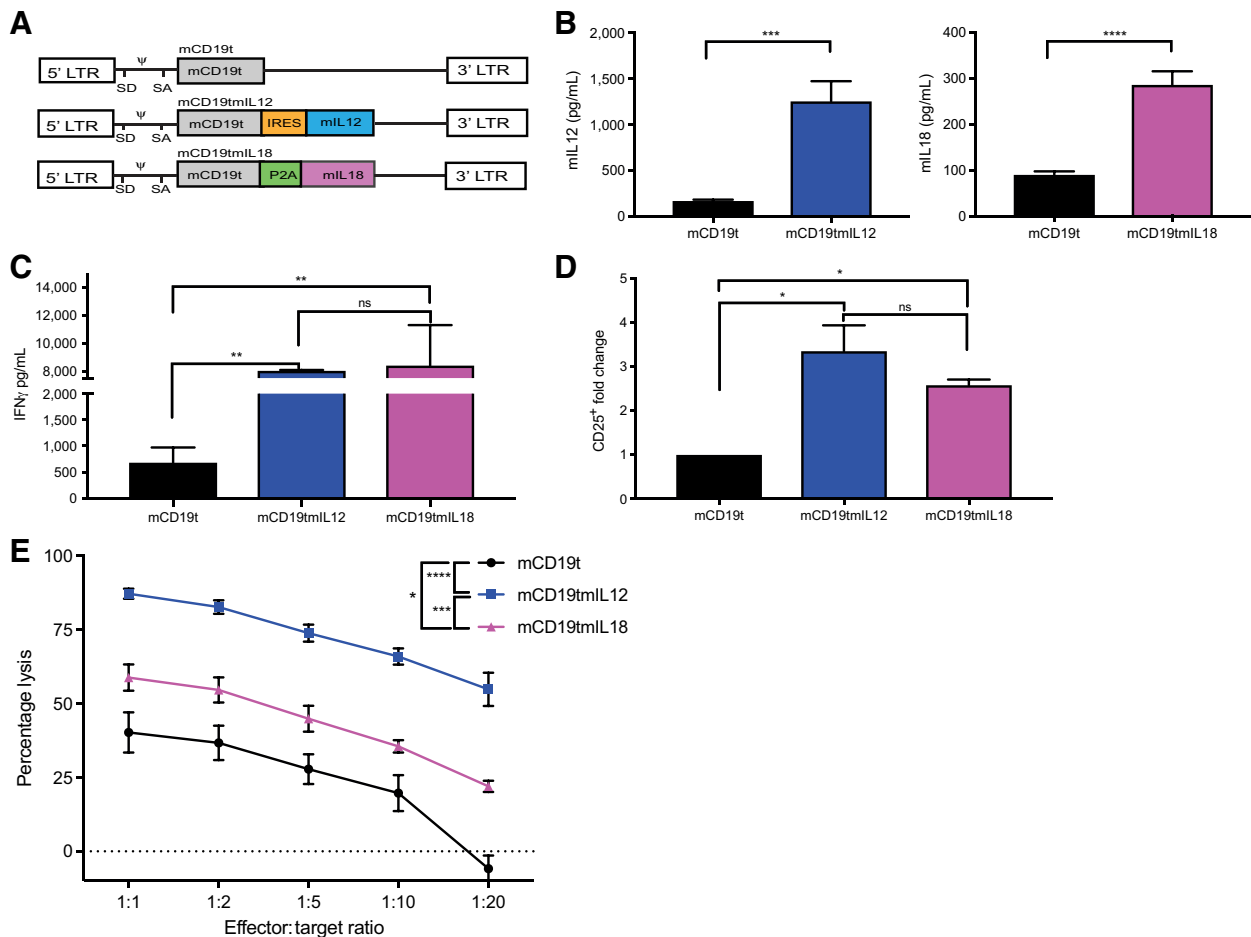
All experiments were performed in accordance with the MSKCC Institutional Animal Care and Use Committee (IACUC)-approved protocol guidelines (MSKCC #00-05-065).

## Results

### IL18 and IL12 enhance the effector function of tumor-specific T cells *in vitro*

Retroviral constructs were generated to armor tumor-specific pmel-1 T cells with proinflammatory cytokines in a syngeneic murine system. Bicistronic constructs were created with a truncated version of murine CD19 (mCD19t) protein to assess transduction efficiency and either a murine IL12  $\alpha$  and  $\beta$  subunit fusion protein (mIL12; ref. 36) or a bioreactive mature version of mIL18 to provide constitutive IL12 or IL18 expression by the long terminal repeat (LTR) promoter (Fig. 1A). Previous work has shown that IL12 secretion after an IRES element limits toxicities (30, 29). Gene transfer of each construct into murine T cells was equivalent (Supplementary Fig. S3A). mCD19tmIL12 and mCD19tmIL18 pmel-1 T cells secreted mIL12 and mIL18, respectively (Fig. 1B).

We next investigated activation and effector function of cytokine-armored pmel-1 T cells through analysis of IFN $\gamma$  secretion, expression of T-cell activation marker CD25, and cytolytic capacity of the transduced T cells after coculture with B16F10 murine melanoma cells. B16F10 cells were negative for costimulatory molecules CD80/

**Figure 1.**

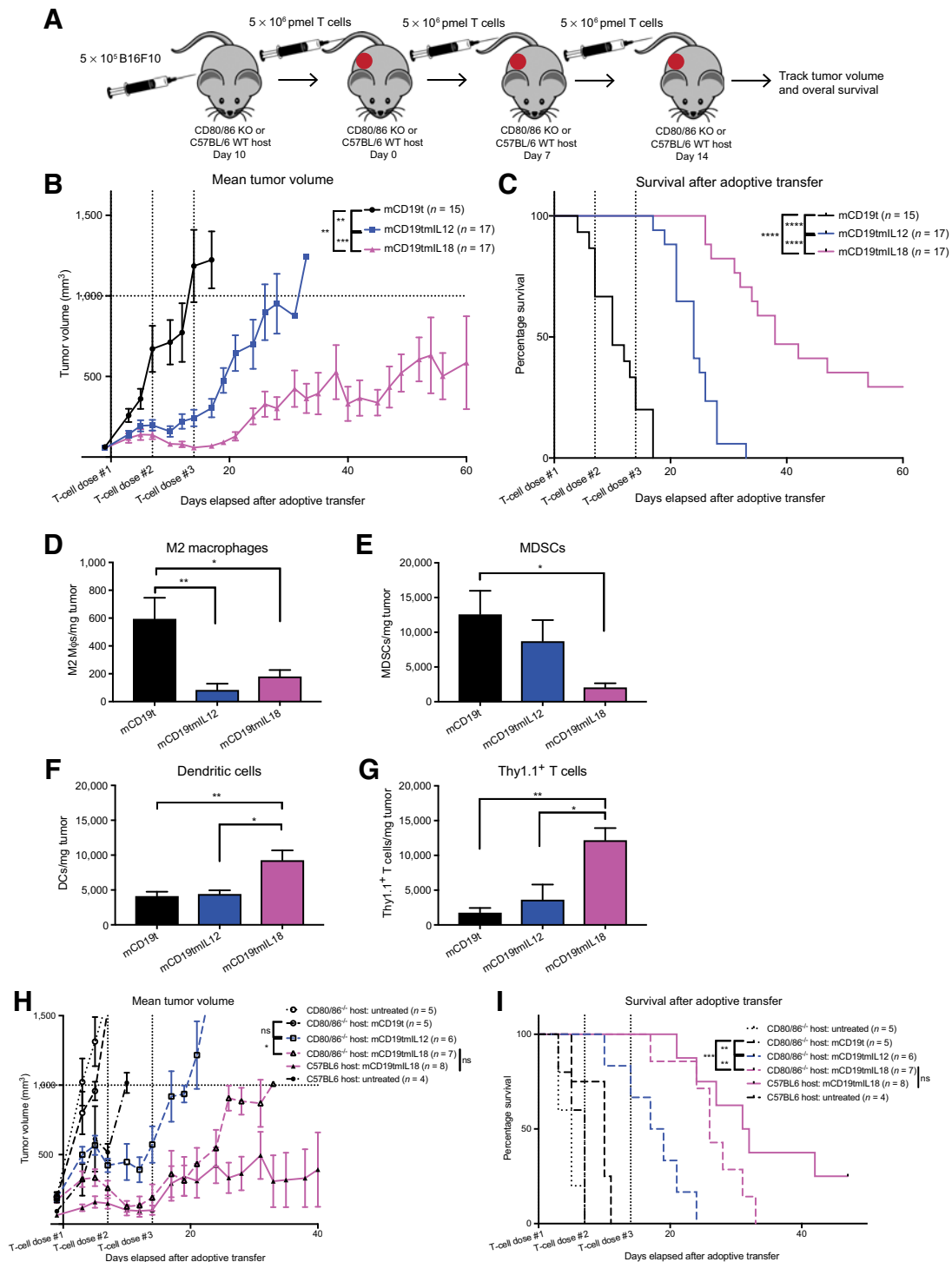
IL18 and IL12 enhance effector function of tumor-specific T cells *in vitro*. **A**, Schematic of retroviral constructs. **B**, Secretion of mIL12 or mIL18 from transduced pmel-1 T cells ( $n = 6$ ; \*\*\*\*,  $P < 0.0001$ ; and \*\*\*,  $P < 0.001$  by unpaired  $t$  tests). Data are mean  $\pm$  SEM of three independent experiments. **C**, IFN $\gamma$  secretion from IL18- or IL12-secreting pmel-1 T cells ( $n = 3$ ; \*\*,  $P < 0.01$  by one-way ANOVA). Data are mean  $\pm$  SD from three independent experiments. **D**, Fold change in CD25 expression, determined by flow cytometry, of armored pmel-1 T cells compared with control following coculture with B16F10 tumor cells. ( $n = 3$ ; \*,  $P < 0.05$  by one-way ANOVA). Data shown are mean  $\pm$  SD from three independent experiments. **E**, *In vitro* cytotoxicity of armored pmel-1 T cells against B16F10 GFP/luc (gp100<sup>+</sup>; CD80/86<sup>-</sup>) tumor cells ( $n = 3$ ; \*\*\*\*,  $P < 0.0001$ ; \*\*\*,  $P < 0.001$ ; and \*,  $P < 0.05$  by one-way ANOVA). Data are mean  $\pm$  SEM of three independent experiments.

CD86 (Supplementary Fig. S3B). Following coculture with B16F10 tumor cells, mIL12- and mIL18-armored pmel-1 T cells displayed enhanced secretion of IFN $\gamma$  (Fig. 1C) and expression of CD25 (Fig. 1D). mIL12 secretion improved the *in vitro* cytolytic capacity of pmel-1 T cells against B16F10 tumor cells modified to express GFP/luciferase (B16F10 GFP/luc) relative to mIL18-secreting pmel-1 T cells and control pmel-1 T cells modified with mCD19t alone (Fig. 1E). mIL18-secreting pmel-1 T cells also enhanced *in vitro* antitumor lysis compared with control pmel-1 T cells (Fig. 1E). These results indicate that both mIL12 and mIL18 augment pmel-1 T-cell activation and effector function *in vitro*.

#### T cells secreting IL18 or IL12 modulate the tumor microenvironment and enhance survival

C57BL/6 mice were inoculated subcutaneously with B16F10 tumor cells and treated weekly for three total infusions with either control or armored pmel-1 T cells to determine T-cell antitumor responses (Fig. 2A). Mice treated with mIL12- or mIL18-armored pmel-1 T cells had a significant delay in tumor growth in compar-

ison with control pmel-1 T cell-treated mice as assessed by tumor volume (Fig. 2B). Mice treated with mIL18-armored pmel-1 T cells were also able to delay tumor growth when compared with mIL12-secreting pmel-1 T cell-treated mice (Fig. 2B). mIL18-armored pmel-1 T cells enhanced overall survival of tumor-bearing mice without preconditioning therapy or exogenous cytokine treatments when compared with mice treated with either mIL12-armored or control pmel-1 T cells (Fig. 2C). The enhanced antitumor effect of the IL18-armored pmel-1 T cells was also evident in tumor-bearing mice treated with a single infusion of pmel-1 T cells (Supplementary Fig. S4A). Tumor samples were isolated from each cohort of treated mice 6 days after a single T-cell infusion for flow cytometric tumor microenvironment analysis. Although there was no difference in the total number of macrophages in the tumor samples among treatment groups (Supplementary Fig. S4B), tumors from mice that received either mIL18- or mIL12-secreting pmel-1 T cells had fewer immunosuppressive CD206<sup>+</sup> M2 macrophages (Fig. 2D; Supplementary Fig. S4C). Only the mice treated with mIL18-secreting armored pmel-1 T cells had significantly fewer CD11b<sup>+</sup>, Ly6C<sup>+</sup>

**Figure 2.**

Adoptively transferred IL18- and IL12-secreting T cells modulate the tumor microenvironment to enhance *in vivo* survival without preconditioning. **A**, *In vivo* experimental protocol. KO, knockout; WT, wild-type. Tumor regression (**B**) and survival (**C**) of C57BL/6 mice bearing established B16F10 tumors and treated with armored or control pmel-1 T cells ( $n = 15-17$ ; \*\*\*\*,  $P < 0.0001$ ; and \*\*,  $P < 0.01$ ).  $P$  values for tumor growth determined by Mann-Whitney test and survival by log-rank Mantel-Cox test, with 95% confidence interval. Data are from three independent experiments. Phenotypic analysis of CD206<sup>+</sup>, Gr1<sup>+</sup>, F4/80<sup>+</sup> M2 macrophages (**D**), CD11b<sup>+</sup>, Ly6C<sup>+</sup> MDSCs (**E**), CD11c<sup>+</sup>, MHC II<sup>+</sup> dendritic cells (DC; **F**), and Thy1.1<sup>+</sup> pmel-1 T cells (**G**) from tumor samples of mice 6 days after T-cell treatment ( $n = 4-8$ ; \*\*,  $P < 0.01$ ; and \*,  $P < 0.05$ ). Data are mean  $\pm$  SEM from two independent experiments and  $P$  values determined by one-way ANOVA. Tumor regression (**H**) and survival (**I**) of CD80/CD86<sup>-/-</sup> and C57BL/6 hosts bearing B16F10 tumors and treated with armored or control pmel-1 T cells ( $n = 4-8$ ; \*\*\*\*,  $P < 0.001$ ; \*\*,  $P < 0.01$ ; and \*,  $P < 0.05$ ).  $P$  values for tumor growth determined by Mann-Whitney test and survival by log-rank Mantel-Cox test, with 95% confidence interval. Data shown are from two independent experiments. ns, not significant.

myeloid-derived suppressor cells (MDSC) in the tumor samples (Fig. 2E; Supplementary Fig. S4C). There was also a significant accumulation of activated MHCII<sup>+</sup> dendritic cells in the tumors of mice treated with mIL18-armed pmel-1 T cells in comparison with the mIL12-armed or control pmel-1 T-cell groups (Fig. 2F; Supplementary Fig. S4C). The decrease in suppressive immune populations within the tumor microenvironment of mIL18-secreting pmel-1 T cells was associated with an enhanced accumulation of pmel-1 T cells (Fig. 2G; Supplementary Fig. S4C) and suggests an explanation for mIL18-armed pmel-1 T cell-mediated control of B16F10 tumors.

To determine the dependency of the enhanced anti-tumor T-cell response upon endogenous CD28 costimulation, we tested the same tumor model in CD80/CD86<sup>-/-</sup> host mice. Nonpreconditioned, tumor-bearing CD80/CD86<sup>-/-</sup> mice treated with mIL18-armed pmel-1 T cells had a slower rate of tumor growth (Fig. 2H) and significantly enhanced survival (Fig. 2I) in comparison with the mIL12-armed and the control pmel-1 T cells. There was no difference in tumor growth or survival between wild-type C57BL/6 or CD80/CD86<sup>-/-</sup> tumor-bearing host mice treated with mIL18-secreting pmel-1 T cells. Thus, IL18 enhanced the efficacy of T-cell therapy in a syngeneic *in vivo* system without preconditioning therapy and irrespective of CD28 T-cell costimulation.

### IL18 supports tumor-specific T cells, whereas IL12 drives T cells into dysfunction

We next investigated activation and *ex vivo* functionality of tumor-specific T cells. Thy1.1<sup>-</sup> host mice were treated with adoptively transferred Thy1.1<sup>+</sup> pmel-1 T cells and tumors were dissected 6 days and 13 days post T-cell infusion (Fig. 3A). On day 6, we observed a significant increase in the ratio of Thy1.1<sup>+</sup> pmel-1 to Thy1.1<sup>-</sup> endogenous T cells only in the mCD19tmIL18 treatment group, indicating an accumulation of mIL18-secreting pmel-1 T cells in the tumor not observed in the mice that were treated with mIL12 or the control pmel-1 T cells (Fig. 3B). There was no difference, however, in naïve/effector/central memory T-cell phenotype among the three treatment groups at the time of infusion or on days 6 or 13 after treatment (Supplementary Fig. S5A). There was no difference in the percentage of PD-1<sup>+</sup>, Thy1.1<sup>+</sup> pmel-1 T cells, illustrating activation of both armored and control pmel-1 T cells (Fig. 3C; Supplementary Fig. S5B). On day 6 after infusion, tumor-infiltrating mIL18-armed pmel-1 T cells had a significantly lower percentage of cells that were triple positive for the inhibitory markers PD-1, TIM-3, and LAG-3 than mIL12-armed pmel-1 T cells (Fig. 3D; Supplementary Fig. S5B). A triple-positive phenotype is a marker of T-cell dysfunction (43). Next we analyzed the CD8<sup>+</sup> effector to CD4<sup>+</sup> helper T-cell ratio in the tumors of mice 6 or 13 days after T-cell treatment. On day 6, there was no difference between the ratio of CD8<sup>+</sup> to CD4<sup>+</sup> T cells in the tumors of mIL12 and mIL18-secreting pmel-1 T cells. On day 13, the ratio of CD8<sup>+</sup> to CD4<sup>+</sup> T cells was higher in tumors of mIL18 pmel-1 T cell-treated mice (Fig. 3E; Supplementary Fig. S5C). Thus, mIL18-secreting CD8<sup>+</sup> pmel-1 T cells retain a functional phenotype and persist at the tumor site after infusion. Conversely, mIL12-secreting pmel-1 T cells develop a dysfunctional phenotype *in vivo* when compared with control or mIL18-armed pmel-1 T cells.

We analyzed the function of tumor-infiltrating pmel-1 T cells on days 6 and 13 by assessing the cytokine production and cytolytic capacity of sorted Thy1.1<sup>+</sup> T cells *ex vivo*. On day 6 after T-cell therapy, both the mIL12 and mIL18 transduced pmel-1 T cells secreted IFN $\gamma$  in comparison with the control pmel-1 T cells (Fig. 3F). On day 13, only

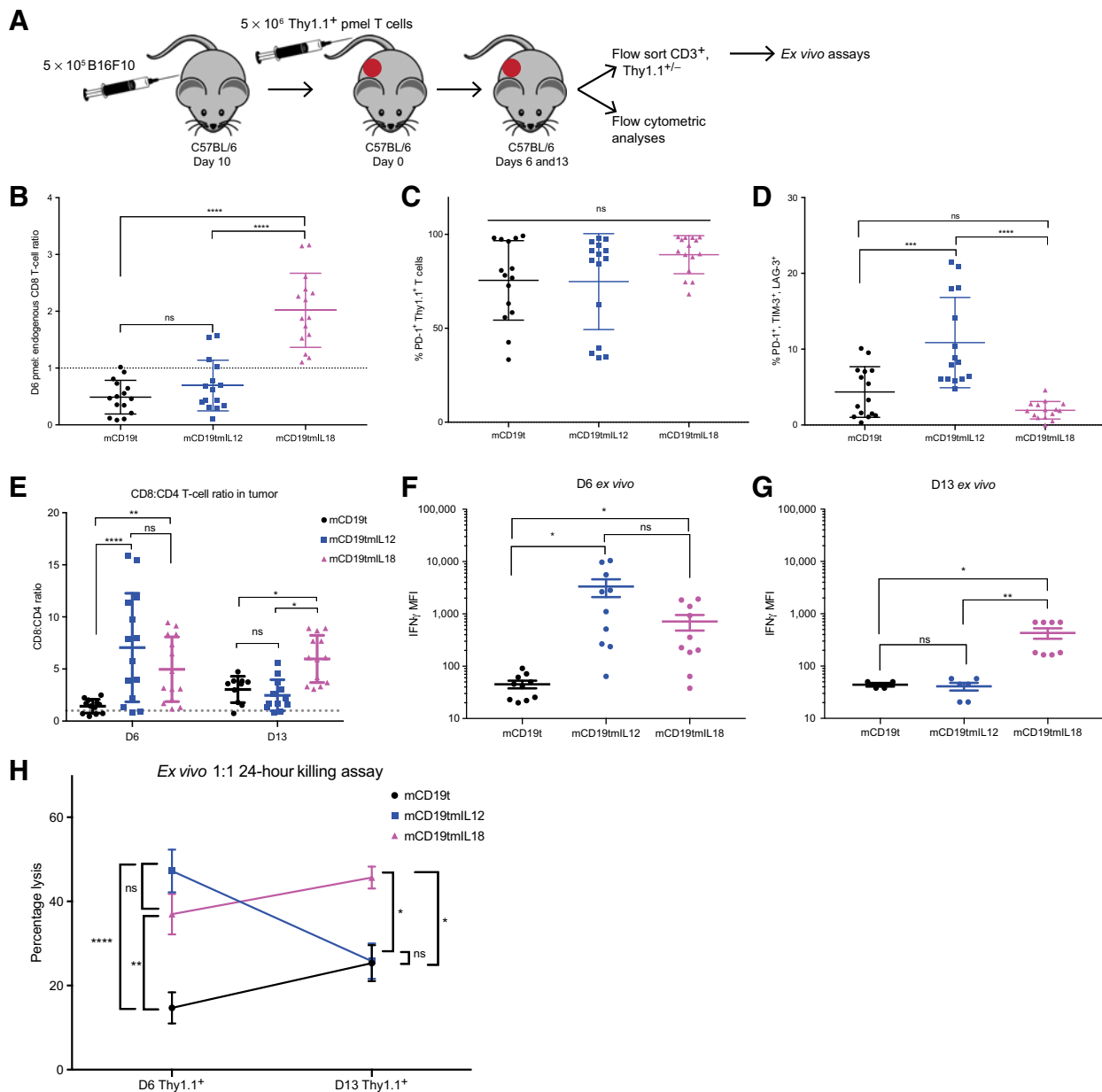
the mIL18-secreting pmel-1 T cells were able to produce more IFN $\gamma$  than the control or the mIL12-secreting pmel-1 T cells (Fig. 3G). Both mIL12 and mIL18 pmel-1 T cells were able to lyse B16F10 GFP/Luc tumor cells on day 6, but only the mIL18 pmel-1 T cells maintained this ability on day 13 (Fig. 3H; Supplementary Fig. S5D). These data align with the phenotypic results described in Fig. 3B–E and demonstrate that mIL18-secreting pmel-1 T cells functionally persist in the tumor longer than the mIL12-secreting pmel-1 T cells, which become dysfunctional.

### IL18-secreting T cells plus sublethal irradiation eradicated established tumors

Although IL18 provides an activating signal and enhances function, persistence, and antitumor efficacy of tumor-specific T cells, long-term survival of mice treated with mIL18-secreting pmel-1 T cells was modest. We hypothesized that combination with sublethal irradiation would have an additive effect and increase survival of tumor-bearing mice due to removal of suppressive cell populations. Sublethally irradiated B16F10 tumor-bearing mice received a single armored or control pmel-1 T-cell injection (Fig. 4A). All T-cell groups displayed equivalent mean fluorescence intensity of mCD19t prior to infusion, demonstrating similar vector expression (Supplementary Fig. S6A). The combination of sublethal irradiation and armored mIL18-secreting pmel-1 T cells regressed the tumors, which were eradicated completely in 8/9 mice (88.8%; Fig. 4B). When sublethal irradiation of tumor-bearing mice was accompanied with three weekly injections of pmel-1 T cells, mIL18-secreting pmel-1 T cells eradicated established subcutaneous tumors (Supplementary Fig. S6B–S6D). In contrast, mice treated with mIL12-secreting pmel-1 T cells in combination with sublethal irradiation succumbed abruptly to toxicity even with mIL12 placed after an IRES element, a strategy meant to limit toxicity (ref. 29; Fig. 4B). Thus, only mice sublethally irradiated and treated with mIL18-secreting pmel-1 T cells survived long term (Fig. 4C).

To confirm that we were observing IL12 toxicity as described previously (25), we analyzed serum cytokines via retro-orbital bleeds from the sublethally irradiated, tumor-bearing mice one week after treatment with the armored or control pmel-1 T cells. The sublethally irradiated, tumor-bearing mice treated with mIL12-secreting pmel-1 T cells had significantly higher amounts of IL12, IFN $\gamma$ , TNF $\alpha$ , IL6, and IL10 in serum in comparison with those mice treated with control mCD19t- or mIL18-secreting pmel-1 T cells (Fig. 4D). On the basis of this cytokine profile, we determined that these mice succumbed to toxicity related to IL12 administration. Taking into consideration both the phenotypic data suggesting that IL18 remains functional for a longer duration as well as the toxicity that developed in sublethally irradiated mice treated with IL12-secreting pmel-1 T cells, we focused further investigation on IL18-secreting T cells.

The enhanced antitumor effect from the combination of pmel-1 T cells with sublethal irradiation was hypothesized to be due to a decrease in suppressive immune cell populations. When compared with the tumors of unconditioned host mice, both CD25<sup>+</sup>, FOXP3<sup>+</sup> regulatory T cells (T<sub>reg</sub>) and CD11b<sup>+</sup>, Ly6G<sup>+</sup> granulocytic MDSCs in the tumors of sublethally irradiated host mice treated with either control pmel-1 T cells or mIL18-secreting pmel-1 T cells were a significantly decreased (Fig. 4E and F; Supplementary Fig. S6E). Although changes in tumor microenvironment were similar in control and mIL18-secreting pmel-1 T cells, a greater number of Thy1.1<sup>+</sup> pmel-1 T cells were detected within the tumors of unconditioned and sublethally irradiated mIL18 pmel-1 T cell-treated

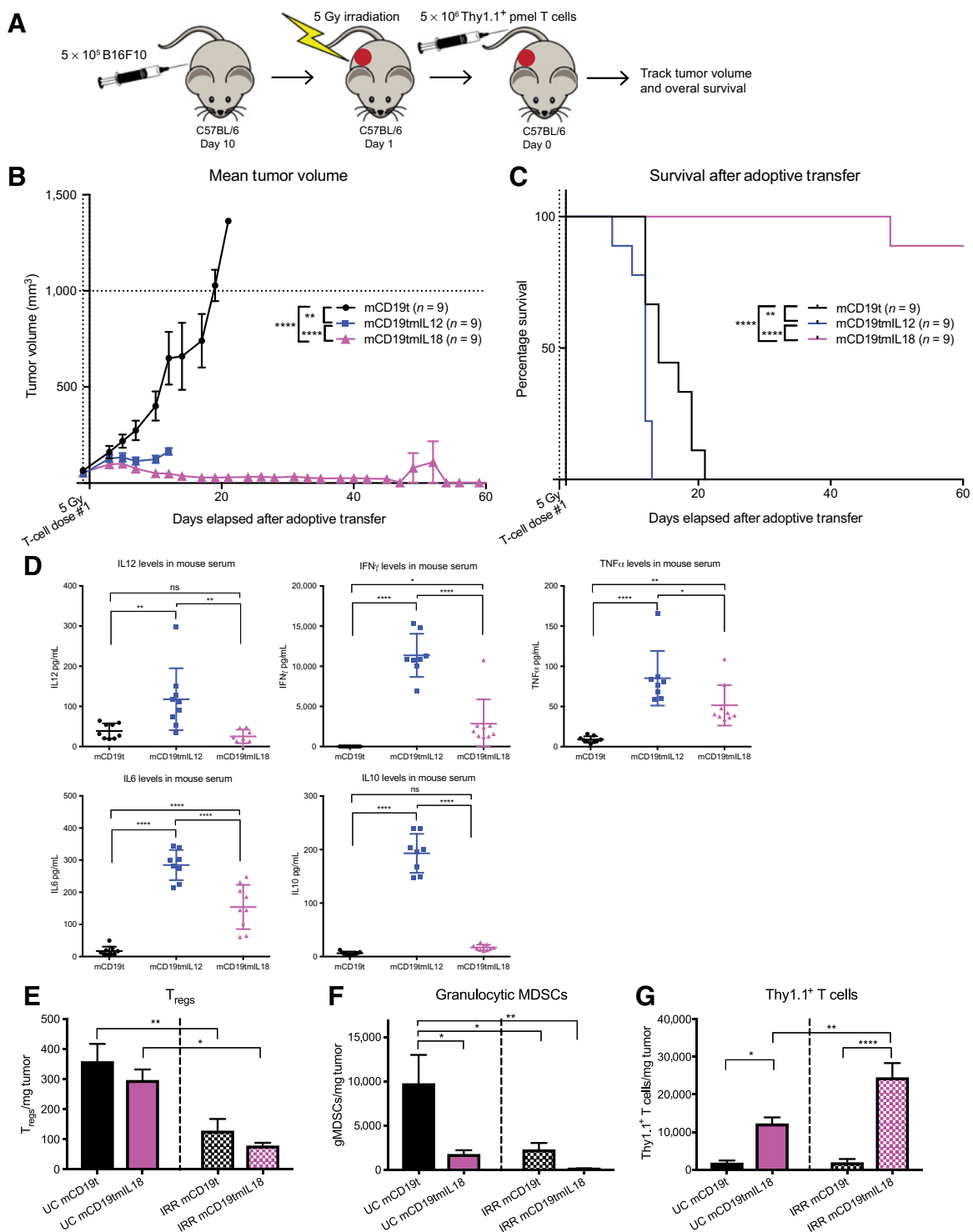
**Figure 3.**

IL18-secreting T cells functionally persist *in vivo*, whereas IL12-secreting T cells become dysfunctional. **A**, Schematic of experimental setup. **B**, Ratio of adoptively transferred pmel-1 Thy1.1<sup>+</sup>, CD8<sup>+</sup> T cells to endogenous Thy1.1<sup>+</sup>, CD8<sup>+</sup> T cells 6 days after T-cell infusion ( $n = 15$ ; \*\*\*\*,  $P < 0.0001$  by one-way ANOVA). Phenotypic analysis of adoptively transferred pmel-1 T cells 6 days after infusion that were single positive for PD-1 as a marker of activation (**C**) or triple positive for exhaustion markers PD-1, LAG-3, and TIM-3 (**D**;  $n = 15$ ; \*\*\*\*,  $P < 0.0001$ ; and \*\*\*,  $P < 0.001$  by one-way ANOVA). **E**, Ratio of CD8<sup>+</sup> to CD4<sup>+</sup> T cells in the tumors of mice 6 or 13 days after treatment with armored or control pmel-1 T cells ( $n = 8-15$ ; \*\*\*\*,  $P < 0.0001$ ; \*\*,  $P < 0.01$ ; and \*,  $P < 0.05$  by two-way ANOVA). Flow cytometry data from three independent experiments and shown mean  $\pm$  SD. *Ex vivo* IFN $\gamma$  production of pmel-1 T cells sorted from tumor samples 6 (**F**) or 13 (**G**) days after treatment with armored or control pmel-1 T cells ( $n = 4-10$ ; \*\*,  $P < 0.01$ ; and \*,  $P < 0.05$  by unpaired *t* test). **H**, *Ex vivo* cytotoxicity of pmel-1 T cells sorted from tumor samples of mice 6 or 13 days after treatment with armored or control pmel-1 T cells ( $n = 7-10$ ; \*\*\*\*,  $P < 0.0001$ ; \*\*,  $P < 0.01$ ; and \*,  $P < 0.05$  by two-way ANOVA). *Ex vivo* data obtained from two independent experiments and shown mean  $\pm$  SEM. MFI, mean fluorescence intensity; ns, not significant.

mice in comparison with control pmel-1 T cell-treated mice (Fig. 4G; Supplementary Fig. S6E). The elimination of suppressive immune populations in the tumors of the mL18 pmel-1 T cell-treated mice with and without sublethal irradiation allowed for enhanced engraftment and persistence of pmel-1 T cells.

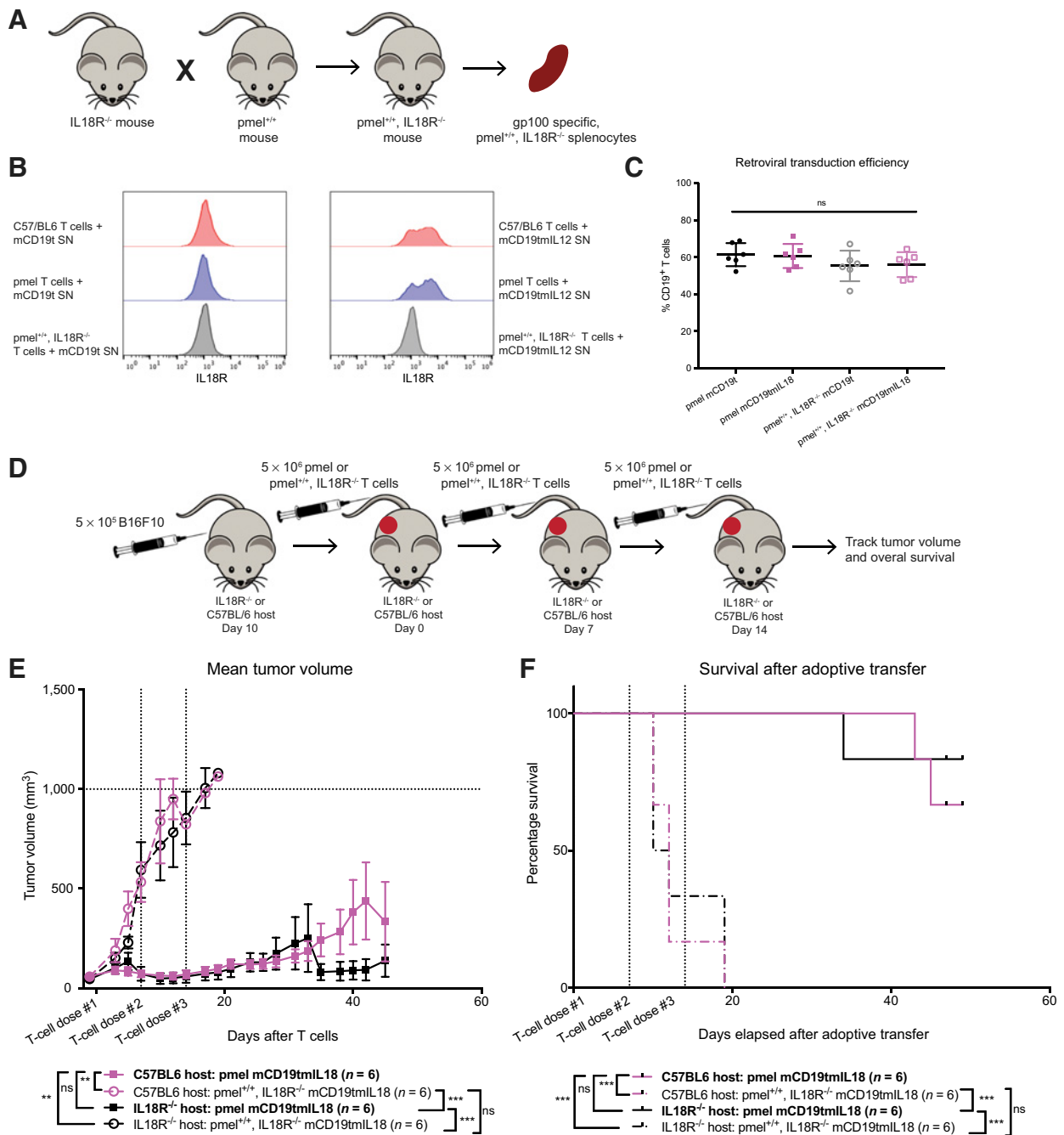
#### IL18-secreting pmel-1 T cells act in *cis* to enhance survival of tumor-bearing mice

Given the antitumor efficacy of mL18-secreting pmel-1 T cells combined with sublethal irradiation, we postulated that IL18 was acting in *cis* on adoptively transferred T cells to mediate an immune

**Figure 4.**

IL18-secreting pmel-1 T cells eradicate established tumors in sublethally irradiated tumor-bearing mice. **A**, *In vivo* experimental protocol. Tumor regression (**B**) and survival (**C**) of C57BL/6 mice bearing established B16F10 tumors and treated with armored or control pmel-1 T cells ( $n = 9$ ; \*\*\*\*,  $P < 0.0001$ ; and \*\*,  $P < 0.01$ ). **D**, Serum cytokine analysis 7 days after T-cell infusion ( $n = 8-9$ ; \*\*\*\*,  $P < 0.0001$ ; \*\*,  $P < 0.01$ ; and \*,  $P < 0.05$ ). Data shown are mean  $\pm$  SD from two independent experiments. Flow cytometry counts of CD25<sup>+</sup>, FOXP3<sup>+</sup> T<sub>regs</sub> (**E**), CD11b<sup>+</sup>, Ly6G<sup>+</sup> granulocytic MDSCs (**F**), and Thy1.1<sup>+</sup> T cells (**G**) in tumors of both unconditioned mice (UC) and sublethally irradiated mice (IRR) 6 days after T-cell infusion ( $n = 4-6$ ; \*\*\*\*,  $P < 0.0001$ ; \*\*,  $P < 0.01$ ; and \*,  $P < 0.05$ ). Data shown are mean  $\pm$  SEM from two independent experiments.  $P$  values for tumor growth determined by Mann-Whitney test, survival determined by log-rank Mantel-Cox test with 95% confidence interval, and cytokine and dissection data determined by one-way ANOVA.



**Figure 5.**

IL18-secreting pmel-1 T cells act in *cis* to enhance *in vivo* survival of tumor-bearing mice. **A**, Schematic of breeding to generate donor pmel<sup>+/+</sup>, IL18R<sup>-/-</sup> mice. **B**, Naïve C57BL/6, pmel, and pmel<sup>+/+</sup>, IL18R<sup>-/-</sup> T cells were cultured with supernatant from either control mCD19t or mCD19tmIL12 pmel-1 T cells. Flow cytometry was used to detect the expression of IL18 receptor on splenocytes. Representative figure of three independent experiments. **C**, Retroviral transduction efficiency by CD19 expression among the experimental groups utilizing either the pmel or pmel<sup>+/+</sup>, IL18R<sup>-/-</sup> T cells ( $n = 6$ ). **D**, *In vivo* experimental protocol. Tumor regression (**E**) and survival (**F**) of C57BL/6 or IL18R<sup>-/-</sup> host mice bearing established B16F10 tumors and treated with armored or control pmel-1 T cells ( $n = 6$ ; \*\*\*,  $P < 0.001$ ; and \*\*,  $P < 0.01$ ).  $P$  values for tumor growth determined by Mann-Whitney test and survival by log-rank Mantel-Cox test, with 95% confidence interval. Data shown are from two independent experiments. ns, not significant.

response. We generated pmel<sup>+/+</sup>, IL18R<sup>-/-</sup> mice as a source of donor T cells by crossing pmel-1 and IL18R<sup>-/-</sup> mice (Fig. 5A). Next, we confirmed via flow cytometry that there was no IL18 receptor present on the naïve pmel<sup>+/+</sup>, IL18R<sup>-/-</sup> donor T cells, even after activation

with supernatant from IL12-secreting pmel-1 T cells, which induces IL18 receptor expression (Fig. 5B). The lack of IL18R did not affect the retroviral transduction efficiency of either the control mCD19t or armored mCD19tmIL18 retroviral constructs in both pmel-1 and

pmel<sup>+/+</sup>, IL18R<sup>-/-</sup> T cells (Fig. 5C). mIL18 secretion improved the *in vitro* cytolytic capacity of only pmel-1 T cells against B16F10 GFP/luc tumor cells relative to control pmel-1 T cells as well as pmel<sup>+/+</sup>, IL18R<sup>-/-</sup> T cells modified with either mIL18 or mCD19t (Supplementary Fig. S7A). This result demonstrated the *cis* effect of IL18 in augmenting *in vitro* T-cell antitumor efficacy.

We asked whether the improved *in vivo* survival of tumor-bearing mice and enhanced antitumor function of mIL18-secreting pmel-1 T cells was dependent on donor T cell or host IL18R expression. In the B16F10 tumor model, both pmel-1 and pmel<sup>+/+</sup>, IL18R<sup>-/-</sup> transduced donor T cells were used to treat C57BL6 or IL18R<sup>-/-</sup> tumor-bearing host mice (Fig. 5D). mIL18-secreting pmel-1 donor T cells delayed tumor progression and enhanced overall survival in both C57BL6 and IL18R<sup>-/-</sup> tumor-bearing mice (Fig. 5E and F). In contrast, the mIL18-secreting pmel<sup>+/+</sup>, IL18R<sup>-/-</sup> donor T cells did not cause tumor regression or prolong survival, similarly to control pmel and pmel<sup>+/+</sup>, IL18R<sup>-/-</sup> treated mice (Fig. 5E and F; Supplementary Fig. S7B and S7C). Antitumor activity is improved regardless of whether IL18R is expressed on the endogenous host immune cells when the mIL18-secreting donor T cell has an intact IL18 receptor. Thus, *cis* interactions between the secreted IL18 and the adoptively transferred T cells are necessary for enhancing antitumor activity.

### Human T cells secreting IL18 enhance survival in a xenograft melanoma model

To demonstrate translational relevance of arming TCR T cells with IL18, we transduced HLA-A2<sup>+</sup> human T cells to express a NY-ESO-1-specific TCR, 1G4, or both the TCR and a mature, bioactive version of hIL18, 1G4hIL18 (Fig. 6A). 1G4 and 1G4hIL18 T cells had similar retroviral transduction efficiency (Supplementary Fig. S8A). 1G4hIL18 T cells significantly enhanced secretion of hIL18 in contrast to mock-transduced and 1G4 T cells (Fig. 6B). After coculture with A375 (HLA-A2<sup>+</sup>, NY-ESO-1<sup>+</sup>) human melanoma cells, both 1G4 and 1G4hIL18 T cells showed enhanced secretion of IFN $\gamma$  and IL2, demonstrating activation of the transduced T cells (Fig. 6C). Both 1G4 and 1G4hIL18 T cells enhanced cell lysis in comparison with mock-transduced T cells when cocultured with A375 tumor cells but not against SK-Mel5 (HLA-A2<sup>+</sup>, NY-ESO-1<sup>-</sup>) tumor cells (Fig. 6D). To confirm this interaction *in vivo*, we utilized an A375 xenograft model of human melanoma and treated with transduced HLA-A2<sup>+</sup> human T cells (Fig. 6E). A375 tumor cells lacked both CD80 and CD86 costimulatory molecules (Supplementary Fig. S8B). Seven days after T-cell infusion, more 1G4hIL18 T cells were present in peripheral blood of the tumor-bearing mice in comparison with both the 1G4 or mock T cell-treated mice (Fig. 6F). 1G4hIL18 T cells delayed tumor progression in comparison with 1G4 and mock-transduced T cells (Fig. 6G). Both 1G4 and 1G4hIL18 T cells enhanced the survival of tumor-bearing mice (Fig. 6H), although the effect was stronger with 1G4hIL18 T cells, showing that IL18 provides a proinflammatory signal to activate human T cells and augment antitumor efficacy through increased persistence of TCR-modified T cells.

## Discussion

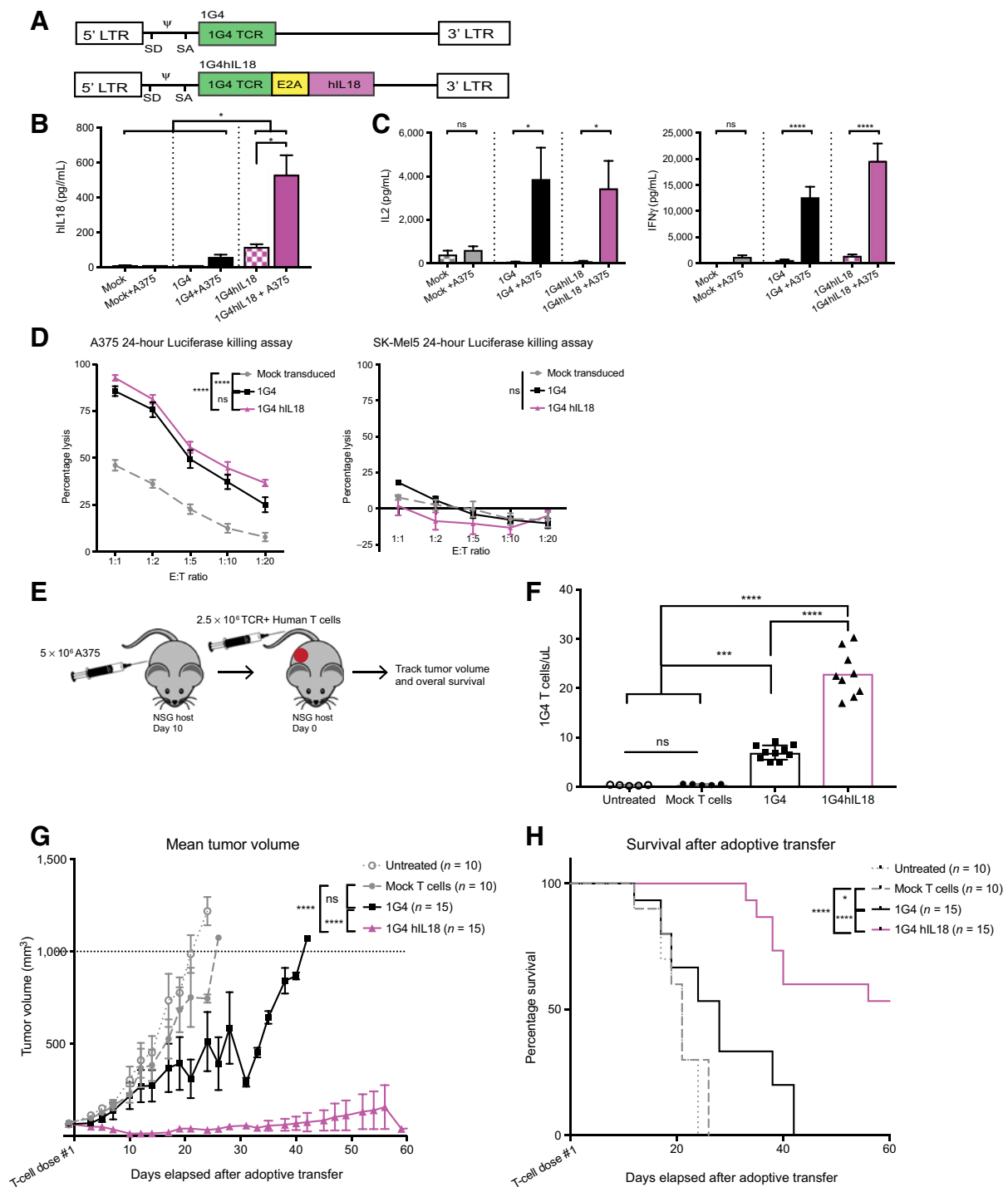
Adoptive cellular therapy with TCR-modified T cells promises to expand the range of targetable tumor-associated antigens, although this strategy has shown only modest success (12–17). Because treatment failure correlates with a lack of T-cell activation, new methods to stimulate tumor-targeted T cells are necessary. In this study, we demonstrated that IL18 provides a proinflammatory signal to T cells.

IL18-engineered TCR-modified T cells promote an enhanced and persistent effector T-cell response by augmenting *in vitro* activation, cytokine release, and tumor lysis of tumor-directed T cells. IL18 promotes a durable activating signal to tumor-specific T cells in both syngeneic and xenograft tumor models. TCR-modified T cells secreting IL18 exhibited enhanced persistence and mediated a delay in tumor growth corresponding to long-term survival of tumor-bearing mice in the absence of any preconditioning therapy by acting *cis* to enhance the effector function of tumor-specific T cells and promote an immunostimulatory tumor microenvironment.

The survival benefit of mIL18-secreting pmel-1 T cells may be due to the reduction of repressive CD206<sup>+</sup> M2 macrophages and MDSCs. The immune microenvironment was conducive to the accumulation of activated dendritic cells and expansion of tumor-specific pmel-1 T cells. This result mirrors that of IL18-secreting CAR T cells which promote a proinflammatory microenvironment with M1 macrophages and activated dendritic cells (31). While IL18 secretion generates a stimulatory tumor microenvironment, the main contribution to the enhanced efficacy of the IL18-secreting TCR-modified T cells is conferred by IL18 acting *cis* on adoptively transferred T cells. Tumor-specific pmel-1 T cells armored with mIL18 functionally persist at the tumor site longer than mIL12-armored pmel-1 T cells that become dysfunctional. *Ex vivo* cytokine secretion and cytolytic assays illustrate that mIL18-secreting pmel-1 T cells remain activated and retain effector function for at least a week longer than mIL12-secreting pmel-1 T cells.

Utilizing pmel<sup>+/+</sup>, IL18R<sup>-/-</sup> donor mice, we established that expression of IL18R on adoptively transferred T cells supports IL18-secreting pmel-1 T cells, regardless of IL18R expression on the endogenous host immune cells. This confirms our hypothesis that the *cis* interactions between the secreted IL18 and the adoptively transferred T cells are essential for enhancing antitumor activity. Although we believe that the *cis* effect of IL18 on the IL18R on adoptively transferred T cells confers the primary antitumor effect, effector cytokines upregulated in the periphery such as IL12, IFN $\gamma$ , and TNF $\alpha$  may play a role in decreasing the suppressive M2 macrophage and MDSC populations. IL12 modulates the murine tumor microenvironment by reducing the number of MDSCs and suppressive macrophages at the tumor site (32). Both IFN $\gamma$  and TNF $\alpha$  proinflammatory cytokines polarize macrophages into a M1-activated phenotype (44–46). From our studies, we have shown that IL18-secreting murine T cells increase the amount of IFN $\gamma$  and TNF $\alpha$  in the periphery, which could be a mechanism by which IL18-secreting T cells polarize macrophages into M1 activated rather than a M2 suppressive phenotype. Any indirect mechanism of suppressive cell depletion may be complementary to the *cis* effect of IL18 on the IL18R on adoptively transferred T cells. The combination of *in vitro*, *in vivo*, and *ex vivo* data demonstrate that secretion of IL18 modulates the tumor microenvironment and provides a more durable proinflammatory signal than IL12 to enhance the antitumor effector function of tumor-specific T cells.

These results with IL18-armored pmel-1 T cells in unconditioned tumor-bearing mice are in contrast to those from other groups which observed modest efficacy of inducible IL18-secreting pmel-1 T cells following multiple methods of chemotherapeutic preconditioning (47) or enhanced toxicity of IL12-armored tumor-specific pmel-1 T cells unless they are under the control of an inducible promoter (33, 47–49). Specifically, a study by Kunert and colleagues, established that T cells transduced with a gp100-specific TCR in combination with an inducible IL18 gene led to antitumor responses in over half of the mice treated when provided in the

**Figure 6.**

Human T cells secreting IL18 persist and enhance survival in a xenograft melanoma model. **A**, Schematic of retroviral constructs. **B**, Luminex results demonstrating secretion of hIL18 by 1G4hIL18 T cells ( $n = 9$ ; \*\*\*,  $P < 0.0001$ ; and \*\*,  $P < 0.001$ ). **C**, Luminex data demonstrating IFN $\gamma$  and IL2 secretion from 1G4 and 1G4hIL18 ( $n = 9$ ; \*\*\*\*,  $P < 0.0001$ ; \*\*\*,  $P < 0.0001$ ; and \*,  $P < 0.05$ ). Luminex data shown as mean  $\pm$  SEM of three independent experiments and  $P$  values determined by one-way ANOVA. **D**, A luciferase killing assay was conducted with 1G4, 1G4hIL18, and mock-transduced human T cells against both A375 (HLA-A2<sup>+</sup>, NY-ESO-1<sup>+</sup>, luciferase<sup>+</sup>) and SK-Mel5 (HLA-A2<sup>+</sup>, NY-ESO-1<sup>-</sup>, luciferase<sup>+</sup>) tumor cells ( $n = 9-15$ ; \*\*\*\*,  $P < 0.0001$  by two-way ANOVA). Data shown are mean  $\pm$  SEM of five independent experiments for A375 and three independent experiments for SK-Mel5 luciferase assay. E:T ratio, effector-to-target ratio. **E**, *In vivo* experimental protocol. **F**, 1G4<sup>+</sup> T-cell numbers in circulation on day 7 after T-cell infusion ( $n = 5-10$ ; \*\*\*\*,  $P < 0.0001$ ; and \*\*\*,  $P < 0.001$  by two-way ANOVA). Tumor regression (**G**) and survival (**H**) of NSG host mice bearing established A375 tumors and treated with armored or control 1G4 human T cells ( $n = 10-15$ ; \*\*\*\*,  $P < 0.0001$ ; and \*,  $P < 0.05$ ). *In vivo* data shown from four independent experiments.  $P$  values for tumor growth determined by Mann-Whitney test and survival by log-rank Mantel-Cox test, with 95% confidence interval. ns, not significant.

context of both bisulfan and cyclophosphamide preconditioning regimens (47). In our studies, pmel-1 T cells transduced to constitutively secrete IL18 combined with sublethal irradiation alone eradicated established tumors in a syngeneic tumor model. This antitumor response was correlated with tumor microenvironment modulation through the ablation of repressive MDSCs and regulatory T cells as well as enhanced engraftment and persistence of tumor-specific T cells within the tumor. In this manner, sublethal irradiation generated a tumor microenvironment devoid of immunosuppressive populations. This suppressive immune cell ablation may augment the stimulatory *cis* interactions of IL18-secreting T cells, leading to this antitumor response. Toxicity was not associated with the IL12-secreting pmel-1 T cells in immune-competent mice. However, after sublethal irradiation preconditioning, we observed fatal toxicity to mice in the form of elevated serum cytokine amounts. Increased IFN $\gamma$  and IL6 has been attributed to cytokine release syndrome toxicities in patients (50) and may have been the effector cytokines that caused the death of the sublethally irradiated mice treated with IL12-secreting pmel-1 T cells.

The syngeneic tumor model data show that TCR-modified T-cell antitumor efficacy can be optimized safely through armoring with IL18 rather than with IL12 and establish IL18 as a superior and safer proinflammatory signal to tumor-directed T cells. These syngeneic studies were used as a proof-of-principle to engineer IL18-armored TCR-modified T cells in a clinically relevant human TCR system. Human T cells were transduced with an anti-NY-ESO-1 TCR. They were then validated and ultimately armored with hIL18. 1G4hIL18 TCR T cells were further shown to persist and enhance antitumor efficacy resulting in long-term survival of tumor-bearing mice in a xenograft model. The NY-ESO-1-directed TCR has been tested in various clinical trials with only modest success (14, 51, 52). Our results provide a rationale for the clinical application of IL18-armored TCR-modified T cells to enhance the efficacy and potency of TCR-modified T-cell therapies.

### Disclosure of Potential Conflicts of Interest

D.J. Drakes has ownership interest in a patent. C.A. Klebanoff is a scientific advisory board member for Achilles Therapeutics, Aleta Biotherapeutics, Bellicum Pharmaceuticals, Obsidian Therapeutics, and Kelun Pharmaceuticals; is a consultant

for G1 Therapeutics and Roche/Genentech; reports receiving commercial research grants from Kite/Gilead and Intima Bioscience; and has ownership interest (including patents) in MSKCC. R.J. Brentjens reports receiving grant support from JUNO Therapeutics (a Bristol-Myers Squibb company); is a consultant/advisor for Gracell Biotechnologies, Inc.; and has ownership interest (including patents) in IL18. No potential conflicts of interest were disclosed by the other authors.

### Authors' Contributions

**Conception and design:** D.J. Drakes, S. Rafiq, C.A. Klebanoff, R.J. Brentjens

**Development of methodology:** D.J. Drakes, S. Rafiq, R.J. Brentjens

**Acquisition of data (provided animals, acquired and managed patients, provided facilities, etc.):** D.J. Drakes, T.J. Purdon, S.S. Chandran, R.J. Brentjens

**Analysis and interpretation of data (e.g., statistical analysis, biostatistics, computational analysis):** D.J. Drakes, S. Rafiq, C.A. Klebanoff, R.J. Brentjens

**Writing, review, and/or revision of the manuscript:** D.J. Drakes, S. Rafiq, C.A. Klebanoff, R.J. Brentjens

**Administrative, technical, or material support (i.e., reporting or organizing data, constructing databases):** D.J. Drakes, A.V. Lopez, C.A. Klebanoff, R.J. Brentjens

**Study supervision:** D.J. Drakes, C.A. Klebanoff, R.J. Brentjens

### Acknowledgments

The authors thank A. Rookard, B. Qeriqi, and C. Bebernitz for technical assistance with *in vivo* experiments; the MSKCC Flow Cytometry Core; J.E. Jaspers, E.L. Smith, and C. Hackett for critically reading the manuscript; and the Klebanoff, Scheinberg, and Wolchok labs for reagents. This work was supported by U.S. NIH grants 5 P01 CA190174-03 (to R.J. Brentjens), 5 P50 CA192937-02 (to R.J. Brentjens), and T32 GM073546-11 (to D.J. Drakes); The Annual Terry Fox Run for Cancer Research (to R.J. Brentjens); Kate's Team (to R.J. Brentjens); Carson Family Charitable Trust (to R.J. Brentjens); Mr. William H. Goodwin and Mrs. Alice Goodwin and the Commonwealth Foundation for Cancer Research (to R.J. Brentjens and C.A. Klebanoff); and the Experimental Therapeutics Center of MSKCC (to R.J. Brentjens, S.S. Chandran, and C.A. Klebanoff). S.S. Chandran and C.A. Klebanoff are also supported by the Parker Institute for Cancer Immunotherapy, the Damon Runyon Cancer Research Foundation, NCI/NIH RFA-CA-18-003 R33, the Breast Cancer Alliance, The Manhasset Women's Coalition Against Breast Cancer, and the MSKCC Core Grant P30 CA008748.

The costs of publication of this article were defrayed in part by the payment of page charges. This article must therefore be hereby marked *advertisement* in accordance with 18 U.S.C. Section 1734 solely to indicate this fact.

Received November 15, 2019; revised January 8, 2020; accepted March 19, 2020; published first March 24, 2020.

### References

- Huse M. The T-cell-receptor signaling network. *J Cell Sci* 2009;22:1269–73.
- Chen L, Flies DB. Molecular mechanisms of T cell co-stimulation and co-inhibition. *Nat Rev Immunol* 2013;13:227–42.
- Schwartz RH. Models of T cell anergy: is there a common molecular mechanism? *J Exp Med* 2004;184:1–8.
- Mueller DL, Jenkins MK. Molecular mechanisms underlying functional T-cell unresponsiveness. *Curr Opin Immunol* 1995;7:375–81.
- Driessens G, Kline J, Gajewski TF. Costimulatory and coinhibitory receptors in anti-tumor immunity. *Immunol Rev* 2009;229:126–44.
- Valenzuela J, Schmidt C, Mescher M. The roles of IL-12 in providing a third signal for clonal expansion of naive CD8 T cells. *J Immunol* 2002;169:6842–9.
- Schmidt CS, Mescher MF. Peptide antigen priming of naive, but not memory, CD8 T cells requires a third signal that can be provided by IL-12. *J Immunol* 2002;168:5521–9.
- Curtsinger JM, Schmidt CS, Mondino A, Lins DC, Kedl RM, Jenkins MK, et al. Inflammatory cytokines provide a third signal for activation of naive CD4+ and CD8+ T cells. *J Immunol* 1999;162:3256–62.
- Curtsinger JM, Mescher MF. Inflammatory cytokines as a third signal for T cell activation. *Curr Opin Immunol* 2010;22:333–40.
- Curtsinger JM, Gerner MY, Lins DC, Mescher MF. Signal 3 availability limits the CD8 T cell response to a solid tumor. *J Immunol* 2007;178:6752–60.
- Chandran SS, Klebanoff CA. T cell receptor-based cancer immunotherapy: emerging efficacy and pathways of resistance. *Immunol Rev* 2019; 290:127–47.
- Morgan RA, Chinnsamy N, Abate-Daga D, Gros A, Robbins PF, Zheng Z, et al. Cancer regression and neurologic toxicity following anti-MAGE-A3 TCR gene therapy. *J Immunother* 2014;36:133–51.
- Morgan RA, Dudley ME, Wunderlich JR, Hughes MS, Yang JC, Sherry RM, et al. Cancer regression in patients after transfer of genetically engineered lymphocytes. *Science* 2006;314:126–9.
- Phan GQ, Rosenberg SA. Adoptive cell transfer for patients with metastatic melanoma: the potential and promise of cancer immunotherapy. *Cancer Control* 2013;20:289–97.
- Zhang J, Wang L. The emerging world of TCR-T cell trials against cancer: a systematic review. *Technol Cancer Res Treat* 2019;18:1533033819831068.
- Tawara I, Kageyama S, Miyahara Y, Fujiwara H, Nishida T, Akatsuka Y, et al. Adoptive transfer of WT1-specific TCR gene-transduced lymphocytes in patients with myelodysplastic syndrome and acute myeloid leukemia. *Blood* 2015;130:1985–94.
- Rohaam MW, van den Berg JH, Kvistborg P, Haanen JBAG. Adoptive transfer of tumor-infiltrating lymphocytes in melanoma: a viable treatment option. *J Immunother Cancer* 2018;6:102.

18. Stevanovic S, Helman SR, Wunderlich JR, Langan MM, Doran SL, Kwong MLM, et al. A phase II study of tumor-infiltrating lymphocyte therapy for human papillomavirus-associated epithelial cancers. *Clin Cancer Res* 2019;25:1486–93.
19. Stauss HJ, Thomas S, Cesco-Gaspere M, Hart DP, Xue SA, Holler A, et al. WT1-specific T cell receptor gene therapy: Improving TCR function in transduced T cells. *Blood Cells Mol Dis* 2008;40:113–6.
20. Linette GP, Stadmauer EA, Maus MV, Rapoport AP, Levine BL, Emery L, et al. Cardiovascular toxicity and titin cross-reactivity of affinity-enhanced T cells in myeloma and melanoma. *Blood* 2013;122:863–71.
21. de Charette M, Marabelle A, Houot R. Turning tumour cells into antigen presenting cells: the next step to improve cancer immunotherapy? *Eur J Cancer* 2016;68:134–47.
22. Seliger B, Mauerer MJ, Ferrone S. Antigen-processing machinery breakdown and tumor growth. *Immunol Today* 2000;21:455–64.
23. Brentjens RJ, Latouche JB, Santos E, Marti F, Gong MC, Lyddane C, et al. Eradication of systemic B-cell tumors by genetically targeted human T lymphocytes co-stimulated by CD80 and interleukin-15. *Nat Med* 2003;9:279–86.
24. Brentjens RJ, Santos E, Nikhamin Y, Yeh R, Matsushita M, La Perle K, et al. Genetically targeted T cells eradicate systemic acute lymphoblastic leukemia xenografts. *Clin Cancer Res* 2007;13:5426–35.
25. Leonard JP, Sherman ML, Fisher GL, Buchanan LJ, Larsen G, Atkins MB, et al. Effects of single-dose interleukin-12 exposure on interleukin-12 associated toxicity and interferon- $\gamma$  production. *Blood* 1997;90:2541–8.
26. Tarhini AA, Millward M, Mainwaring P, Kefford R, Logan T, Pavlick A, et al. A phase 2, randomized study of SB-485232, rhIL-18, in patients with previously untreated metastatic melanoma. *Cancer* 2009;115:859–68.
27. Dinarello CA, Novick D, Kim S, Kaplanski G. Interleukin-18 and IL-18 binding protein. *Front Immunol* 2013;4:289.
28. Wu C, Sakorafas P, Miller R, McCarthy D, Scesney S, Dixon R, et al. IL-18 receptor  $\beta$ -induced changes in the presentation of IL-18 binding sites affect ligand binding and signal transduction. *J Immunol* 2003;170:5571–7.
29. Pegram HJ, Lee JC, Hayman EG, Imperato GH, Tedder TF, Sadelain M, et al. Tumor-targeted T cells modified to secrete IL-12 eradicate systemic tumors without need for prior conditioning. *Blood* 2012;119:4133–41.
30. Yeku OO, Purdon TJ, Koneru M, Spriggs D, Brentjens RJ. Armored CAR T cells enhance antitumor efficacy and overcome the tumor microenvironment. *Sci Rep* 2017;7:1–14.
31. Avanzi MP, Yeku O, Li X, Wijewarnasuriya DP, van Leeuwen DG, Cheung K, et al. Engineered tumor-targeted T cells mediate enhanced anti-tumor efficacy both directly and through activation of the endogenous immune system. *Cell Rep* 2018;23:2130–41.
32. Kerkar SP, Muranski P, Kaiser A, Boni A, Sanchez-Perez L, Yu Z, et al. Tumor-specific CD8+ T cells expressing interleukin-12 eradicate established cancers in lymphodepleted hosts. *Cancer Res* 2010;70:6725–34.
33. Zhang L, Kerkar SP, Yu Z, Zheng Z, Yang S, Restifo NP, et al. Improving adoptive T cell therapy by targeting and controlling IL-12 expression to the tumor environment. *Mol Ther* 2011;19:751–9.
34. Overwijk WW, Theoret MR, Finkelstein SE, Surman DR, de Jong LA, Vyth-Dreese FA, et al. Tumor regression and autoimmunity after reversal of a functionally tolerant state of self-reactive CD8+ T cells. *J Exp Med* 2003;198:569–80.
35. Rivière I, Brose K, Mulligan RC. Effects of retroviral vector design on expression of human adenosine deaminase in murine bone marrow transplant recipients engrafted with genetically modified cells. *Proc Natl Acad Sci U S A* 1995;92:6733–7.
36. Ferrone CR, Perales MA, Goldberg SM, Somberg CJ, Hirschhorn-Cyerman D, Gregor PD, et al. Adjuvanticity of plasmid DNA encoding cytokines fused to immunoglobulin Fc domains. *Clin Cancer Res* 2006;12:5511–9.
37. Wargo JA, Robbins PF, Li Y, Zhao Y, El-Gamil M, Caragacianu D, et al. Recognition of NY-ESO-1+ tumor cells by engineered lymphocytes is enhanced by improved vector design and epigenetic modulation of tumor antigen expression. *Cancer Immunol Immunother* 2009;58:383–94.
38. Cohen CJ. Enhanced antitumor activity of murine-human hybrid T-cell receptor (TCR) in human lymphocytes is associated with improved pairing and TCR/CD3 stability. *Cancer Res* 2006;66:8878–86.
39. Cohen CJ, Li YF, El-Gamil M, Robbins PF, Rosenberg SA, Morgan RA. Enhanced antitumor activity of T cells engineered to express T-cell receptors with a second disulfide bond. *Cancer Res* 2007;67:3898–903.
40. Lee J, Sadelain M, Brentjens R. Retroviral transduction of murine primary T lymphocytes. *Methods Mol Biol* 2009;506:83–96.
41. Rafiq S, Purdon TJ, Daniyan AF, Koneru M, Dao T, Liu C, et al. Optimized T-cell receptor-mimic chimeric antigen receptor T cells directed toward the intracellular Wilms tumor 1 antigen. *Leukemia* 2017;31:1788–97.
42. Smith EL, Staehr M, Masakayan R, Tataka IJ, Purdon TJ, Wang X, et al. Development and evaluation of an optimal human single-chain variable fragment-derived BCMA-targeted CAR T cell vector. *Mol Ther* 2018;26:1447–56.
43. Gros A, Robbins PF, Yao X, Li YF, Turcotte S, Tran E, et al. PD-1 identifies the patient-specific CD8+ tumor-reactive repertoire infiltrating human tumors. *J Clin Invest* 2014;124:2246–59.
44. Martinez FO, Gordon S. The M1 and M2 paradigm of macrophage activation: time for reassessment. *F1000Prime Rep* 2014;6:13.
45. Gordon S, Martinez FO. Alternative activation of macrophages: mechanism and functions. *Immunity* 2010;32:593–604.
46. Stein M, Keshav S, Harris N, Gordon S. Interleukin 4 potentially enhances murine macrophage mannose receptor activity: a marker of alternative immunologic macrophage activation. *J Exp Med* 1992;176:287–92.
47. Kunert A, Chmielewski M, Wijers R, Berrevoets C, Abken H, Debets R. Intratumoral production of IL18, but not IL12, by TCR-engineered T cells is non-toxic and counteracts immune evasion of solid tumors. *Oncoimmunology* 2017;7:e1378842.
48. Yamamoto TN, Lee PH, Vodnala SK, Gurusamy D, Kishton RJ, Yu Z, et al. T cells genetically engineered to overcome death signaling enhance adoptive cancer immunotherapy. *J Clin Invest* 2019;129:1551–65.
49. Restifo NP, Dudley ME, Rosenberg SA. Adoptive immunotherapy for cancer: harnessing the T cell response. *Nat Rev Immunol* 2012;12:269–81.
50. Grupp SA, Kalos M, Barrett D, Aplenc R, Porter DL, Rheingold SR, et al. Chimeric antigen receptor-modified T cells for acute lymphoid leukemia. *N Engl J Med* 2013;368:1509–18.
51. Thomas R, Al-Khadairi G, Roelands J, Hendrickx W, Dermime S, Bedognetti D, et al. NY-ESO-1 based immunotherapy of cancer: current perspectives. *Front Immunol* 2018;9:947.
52. D'Angelo SP, Melchiori L, Merchant MS, Bernstein D, Glod J, Kaplan R, et al. Antitumor activity associated with prolonged persistence of adoptively transferred NY-ESO-1c259T cells in synovial sarcoma. *Cancer Discov* 2018;8:944–57.

# Cancer Immunology Research

## Optimization of T-cell Receptor–Modified T Cells for Cancer Therapy

Dylan J. Drakes, Sarwish Rafiq, Terence J. Purdon, et al.

*Cancer Immunol Res* Published OnlineFirst March 24, 2020.

<b>Updated version</b>	Access the most recent version of this article at: doi: <a href="https://doi.org/10.1158/2326-6066.CIR-19-0910">10.1158/2326-6066.CIR-19-0910</a>
<b>Supplementary Material</b>	Access the most recent supplemental material at: <a href="http://cancerimmunolres.aacrjournals.org/content/suppl/2020/03/24/2326-6066.CIR-19-0910.DC1">http://cancerimmunolres.aacrjournals.org/content/suppl/2020/03/24/2326-6066.CIR-19-0910.DC1</a>

**E-mail alerts** [Sign up to receive free email-alerts](#) related to this article or journal.

**Reprints and Subscriptions** To order reprints of this article or to subscribe to the journal, contact the AACR Publications Department at [pubs@aacr.org](mailto:pubs@aacr.org).

**Permissions** To request permission to re-use all or part of this article, use this link <http://cancerimmunolres.aacrjournals.org/content/early/2020/05/06/2326-6066.CIR-19-0910>. Click on "Request Permissions" which will take you to the Copyright Clearance Center's (CCC) Rightslink site.